

# New approaches to quantifying aerosol influence on the cloud radiative effect

Graham Feingold<sup>a,1</sup>, Allison McComiskey<sup>b</sup>, Takano Yamaguchi<sup>a,c</sup>, Jill S. Johnson<sup>d</sup>, Kenneth S. Carslaw<sup>d</sup>, and K. Sebastian Schmidt<sup>e</sup>

<sup>a</sup>Chemical Sciences Division, Earth System Research Laboratory, National Oceanic and Atmospheric Administration, Boulder, CO 80305; <sup>b</sup>Global Monitoring Division, Earth System Research Laboratory, National Oceanic and Atmospheric Administration, Boulder, CO 80305; <sup>c</sup>Cooperative Institute for Research in Environmental Sciences, University of Colorado Boulder, Boulder, CO 80309; <sup>d</sup>Institute for Climate and Atmospheric Science, School of Earth and Environment, University of Leeds, Leeds LS2 9JT, United Kingdom; and <sup>e</sup>Laboratory for Atmospheric and Space Physics, University of Colorado Boulder, Boulder, CO 80303

Edited by John H. Seinfeld, California Institute of Technology, Pasadena, CA, and approved November 3, 2015 (received for review August 18, 2015)

**The topic of cloud radiative forcing associated with the atmospheric aerosol has been the focus of intense scrutiny for decades. The enormity of the problem is reflected in the need to understand aspects such as aerosol composition, optical properties, cloud condensation, and ice nucleation potential, along with the global distribution of these properties, controlled by emissions, transport, transformation, and sinks. Equally daunting is that clouds themselves are complex, turbulent, microphysical entities and, by their very nature, ephemeral and hard to predict. Atmospheric general circulation models represent aerosol–cloud interactions at ever-increasing levels of detail, but these models lack the resolution to represent clouds and aerosol–cloud interactions adequately. There is a dearth of observational constraints on aerosol–cloud interactions. We develop a conceptual approach to systematically constrain the aerosol–cloud radiative effect in shallow clouds through a combination of routine process modeling and satellite and surface-based shortwave radiation measurements. We heed the call to merge Darwinian and Newtonian strategies by balancing microphysical detail with scaling and emergent properties of the aerosol–cloud radiation system.**

aerosol | cloud | radiation | climate forcing

The climate system, with its couplings between land surface, vegetation, ocean, cryosphere, and atmosphere, is an extraordinarily complex system that is under intensive scrutiny for the purposes of climate analysis and prediction. The atmospheric aerosol and its interaction with clouds is a poorly quantified component of the climate system and is the focus of the current study. The aerosol comprises suspended particles that derive from the oceans, land surface, volcanoes, and anthropogenic activities. The difficulty in quantifying climate forcing by the aerosol emanates partly from the complexity in the aerosol itself, and partly from the fact that its influence on clouds requires detailed understanding of clouds and cloud feedbacks at a range of spatio-temporal scales. Untangling the multiple cloud responses that occur as a result of aerosol perturbations is particularly difficult (1). As one example, consider the influence of the aerosol on clouds and precipitation. Assuming no change in condensed water, the aerosol, by acting as nucleation sites for droplets, might generate smaller droplets, more reflective clouds (2), and reduced precipitation (3). However, through a multitude of complex and contingent pathways, aerosol-perturbed clouds sometimes appear to have similar reflectance because brightening is offset by reductions in cloud water, a fundamental property controlling cloud reflectance. On short timescales (hours), the aerosol tends to reduce precipitation in shallow, liquid-only clouds, but this may be offset over longer periods (multiple days) (4). Deep, mixed-phase convective clouds present even more complex pathways for generation of precipitation, and even more contingencies. The aerosol appears to change the distribution and intensity of surface rain from deep convective clouds (5); however, longer timescale drivers (weeks to months) associated with radiative heating and long-term

modification to the surface fluxes by the aerosol could be equally if not more important (6, 7).

## Paradigms in Pursuit of Quantification of the Cloud Radiative Effect

The immense complexity of the aerosol itself, the sensitivity of clouds to both meteorological controls and the aerosol, and the covariability of rapidly changing clouds and aerosol present a particularly challenging problem. As in other studies of complex systems, researchers tend to separate based on academic tradition or discipline into those with a “Newtonian” outlook and those who take a “Darwinian” approach. To paraphrase Harte (8), the Newtonian stresses, among others, fundamental physical laws, a search for patterns, simple models, and predictive capability based on initial conditions and deterministic laws of physics. In contrast, the Darwinian is more cognizant of the system complexity and contingencies, opposes simple models, and addresses smaller, more manageable, or unique pieces of the problem. Harte has argued eloquently for a synthesis of these two approaches for Earth system science. We will attempt to argue the same as a means of advancing our understanding of, and ability to quantify, the cloud radiative effect (CRE). [CRE refers to the difference between “all-sky” (cloudy + clear sky) and “clear-sky” radiation at a given time. In contrast, “radiative forcing” refers to present-day minus pre-industrial influence of a given constituent.] Threads of this thinking date even earlier, to Karl Popper’s work on physical determinism and human behavior, eloquently presented in an essay entitled “Of Clocks and Clouds” (9) in which he describes complex systems in terms of either “clock-like,” predictable systems based on fundamental rules or “cloud-like” systems characterized by “fuzziness” and unpredictability. Our (open) aerosol–cloud system is, by definition, nebulous and fuzzy, but is nevertheless based on fundamental physics. As in Popper’s world, it is characterized by neither pure physical determinism nor pure chaos. Describing it fully therefore requires a synergy of these approaches. In Popper’s words “What we need for understanding rational human behaviour... is something intermediate in character between perfect chance and perfect determinism; something intermediate

This paper results from the Arthur M. Sackler Colloquium of the National Academy of Sciences, “Improving Our Fundamental Understanding of the Role of Aerosol–Cloud Interactions in the Climate System,” held June 23–24, 2015, at the Arnold and Mabel Beckman Center of the National Academies of Sciences and Engineering in Irvine, CA. The complete program and video recordings of most presentations are available on the NAS website at [www.nasonline.org/Aerosol\\_Cloud\\_Interactions](http://www.nasonline.org/Aerosol_Cloud_Interactions).

Author contributions: G.F., A.M., T.Y., J.S.J., and K.S.C. designed research; G.F., A.M., T.Y., and K.S.S. performed research; J.S.J., K.S.C., and K.S.S. contributed new reagents/analytic tools; G.F. and T.Y. analyzed data; and G.F. and A.M. wrote the paper.

The authors declare no conflict of interest.

This article is a PNAS Direct Submission.

<sup>1</sup>To whom correspondence should be addressed. Email: [graham.feingold@noaa.gov](mailto:graham.feingold@noaa.gov).

This article contains supporting information online at [www.pnas.org/lookup/suppl/doi:10.1073/pnas.1514035112/-DCSupplemental](http://www.pnas.org/lookup/suppl/doi:10.1073/pnas.1514035112/-DCSupplemental).

between perfect clouds and perfect clocks.” We argue that the same is true for complex physical systems.

Our motivation is twofold: (i) to improve our understanding of cloud-controlling parameters and cloud albedo-controlling parameters with a goal of improving representation of these processes in atmospheric general circulation models (AGCMs) and (ii) to enable observational quantification of the aerosol–cloud radiative effect with a focus on process-level understanding. This paper will offer a retrospective of some older approaches to quantification, together with some new ones, to illustrate how the community might reorganize how it thinks about the aerosol–cloud problem. The ideas herein draw on many in the published literature, so this work stresses methodology rather than novelty.

To present our ideas, we deal solely with warm (liquid water) clouds, whose dominant influence on radiation is in the short-wave (SW), and for which there is abundant qualitative evidence but insufficient quantification of an aerosol influence.

### Examples

Within subdisciplines, researchers have traditionally focused on fundamental understanding by addressing parts of the problem. However, the interactions among these components and the implications for climate-scale phenomena lend themselves to broader consideration of the environment in which the clouds evolve (dynamics), and the couplings between dynamics, aerosol/cloud microphysics, and radiation. Twomey’s (2) landmark paper on aerosol brightening of clouds drove a generation of scientists to try to quantify cloud brightening, whereas, today, the focus has shifted to the dynamical adjustments of the system that occur in response to such brightening, and whether they amplify (3) or diminish (1, 10) such brightening.

Just a few decades ago, it was common to use a cloud model to study a single cloud cell or a subset of cloud processes (Darwinian), whereas, today, one can simulate a field of clouds based on the same fundamental physics and attempt to project results onto other cloud systems (Newtonian). However, in adding more physics and process interactions, the system rapidly becomes complex enough that the Newtonian approach falls short of being fully explanatory or able to untangle all causal relationships. The “tug of war” between fundamental physics projected to the system and system-wide behavior that has driven detailed analysis of subcomponents of the system can be exemplified in the following. Suppose one would like to quantify the relationship between planetary albedo ( $R$ ) and aerosol emissions ( $E$ ). An equation for this relationship can be broken down via the Chain Rule (11) as

$$\Delta R = R \frac{d \ln R}{d \ln \tau} \frac{d \ln \tau}{d \ln N_d} \frac{d \ln N_d}{d \ln \text{CCN}} \frac{d \ln \text{CCN}}{d \ln E} \Delta \ln E \quad [1]$$

where  $\tau$  is cloud optical depth,  $N_d$  is drop concentration, and CCN is cloud condensation nucleus concentration. [This equation assumes a cloudy column; i.e., there is no influence of the aerosol on cloud fraction. While this is unrealistic, the equation is simply used to expound an idea (presented below) rather than for purposes of quantification.] Depending on discipline and expertise, the community has coalesced around quantifying individual components of this expansion, both in models, as a means of identifying differences between model representations of said components in a present-day minus preindustrial sense, and through observations, where the terms are assessed based on present-day measurements. [The relationship between radiative forcing and effect could be addressed with a kernel method (12). The assumption that radiative forcing calculated based on present-day aerosol–cloud interactions is equivalent to forcing based on present-day minus pre-industrial aerosol might result

in a low bias in forcing (13).] Addressing any given component of Eq. 1 requires further expansion, e.g.,

$$\frac{d \ln \tau}{d \ln N_d} = \frac{1}{3} \left[ 1 + 2 \frac{d \ln L}{d \ln N_d} + \frac{d \ln k}{d \ln N_d} + 3 \frac{d \ln H}{d \ln N_d} \right] \quad [2]$$

where  $L$  is liquid water path,  $k$  represents drop size distribution breadth, and  $H$  is cloud depth. Like the progressive unpeeling of layers of an onion, these terms themselves require further expansion and quantification. Unfortunately, the nature of our measurement systems means that there are large uncertainties associated with the terms in Eq. 2, in magnitude and even in sign. Physical retrievals of the various parameters are often fraught with instrumental or measurement error and assumptions. Individual terms are poorly constrained, and errors compound to yield great uncertainty. For example, in ref. 14, the authors state that although their data generally conform to the expansion in Eq. 2 quite well, they do so because of compensating errors in individual terms. In addition, the sometimes disparate measurement scales, and scales of aggregation associated with different platforms or instruments, can further confound quantification (15). Given our current ability to quantify through observations the components in Eqs. 1 and 2, if Eq. 1 or some subcomponent like Eq. 2 were to match a proposed theory, how confident could one be in the suitability of that theory?

An alternative approach is to shift attention to observations of system-wide variables that are more closely related to CRE, and for which uncertainties are better known. One example is the relationship between scene albedo  $A$  (cloudy plus clear sky portions) and cloud fraction  $f_c$ , expressed as (16, 17)

$$A = A_c f_c + A_s (1 - f_c), \quad [3]$$

where  $A_c$  is cloud albedo and  $A_s$  is surface albedo.  $A_c$  is itself a function of  $\tau$ , and therefore  $L$  and  $N_d$ . Approximately linear relationships between MODIS (Moderate Resolution Imaging Spectroradiometer)-derived  $f_c$  and CERES (Clouds and the Earth’s Radiant Energy System)-derived  $A$  in multiple marine stratocumulus locations have been found when averaging over  $2.5^\circ \times 2.5^\circ$  and 1-mo periods (18). (Based on Eq. 3, linearity suggests an independence of  $A_c$  and  $f_c$ .) Regardless of the exact form, the ( $A, f_c$ ) relationship has distinct advantages: It can be addressed with fewer measurements than the Chain Rule expansions, measurement error and uncertainty are more directly linked to CRE, measurements can be made from space and from the ground (19, 20), and it captures important underlying physics (21, 22). It is currently used as a means of diagnosing AGCM performance (17, 18) but, as we will argue below, could be applied to process models as well.

The ( $A, f_c$ ) relationship therefore provides a key element of the merged Newtonian–Darwinian approach, i.e., it is an expression of scaling (Harte’s “search for patterns and laws”). However, does it exhibit another very desirable property, namely self-similarity or scale-independence, e.g., does the ( $A, f_c$ ) relationship vary with spatial or temporal averaging scale? Does it vary across cloud regimes? If so, can one directly trace the variability to physical processes? Some of these themes will be addressed, albeit briefly, below.

One might argue that in examining relationships such as ( $A, f_c$ ) rather than ( $\tau, N_d$ ), we are simply shifting the unknown(s) elsewhere. We counter that assessing uncertainties in a higher-level relationship like ( $A, f_c$ ) is more productive than getting entangled in similar uncertainties in lower-order relationships. Are we abrogating our fundamental intellectual need or mandate to understand and predict all subcomponents of the system? We argue that the broader view, in combination with an appropriate balance of process-level understanding, has been particularly productive in other fields. As an illustration, consider the study of “emergence,” another nexus of the Newtonian and Darwinian approaches. Complex pattern formation sometimes emerges from

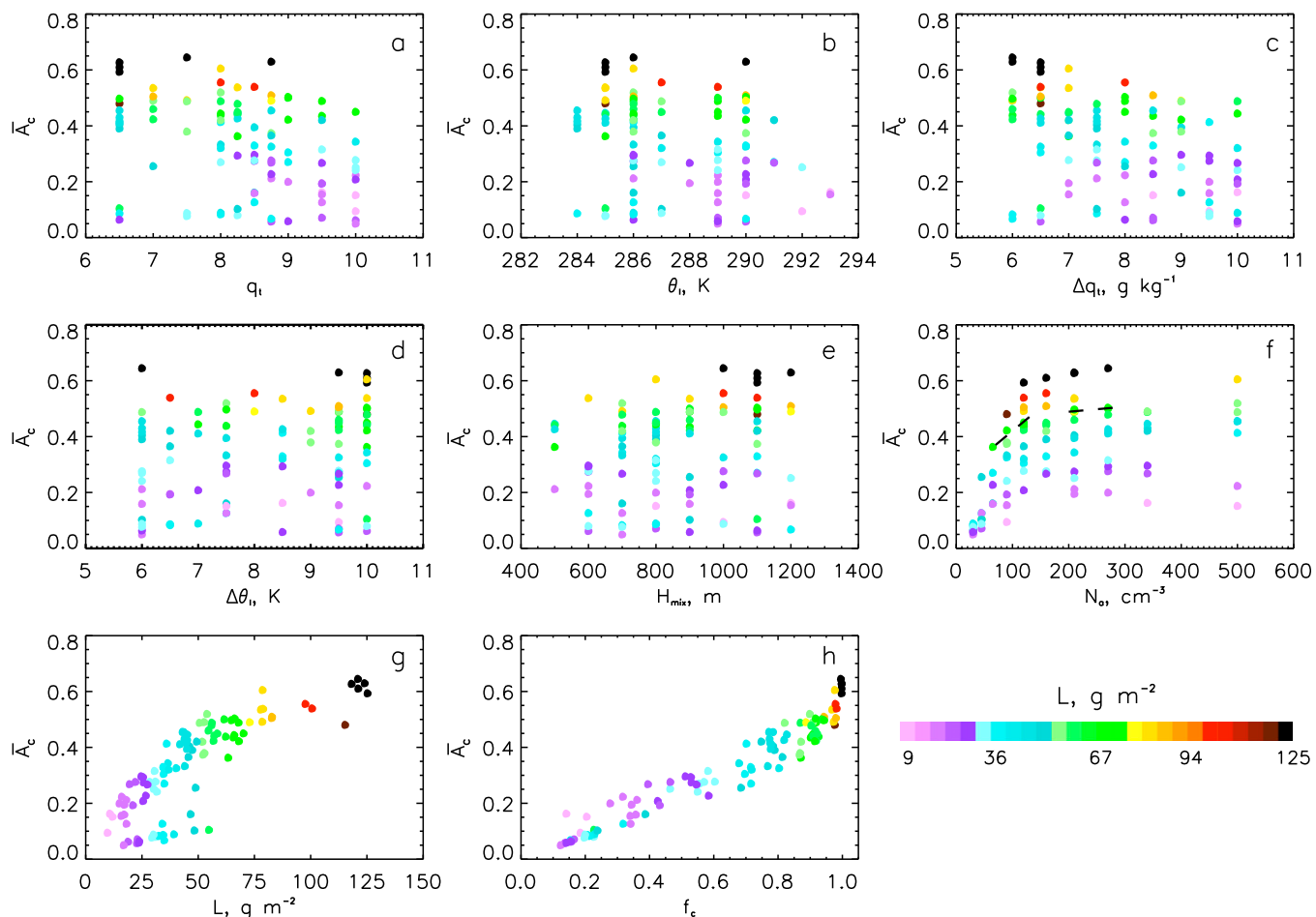


**Fig. 1.** Scatterplot of domain mean cloud albedo  $\bar{A}_c$  (sum of  $A_c$  normalized by number of columns in domain) as a function of input conditions (A)  $q_t$ , (B)  $\theta_l$ , (C)  $\Delta q_t$ , (D)  $\Delta\theta_l$ , (E)  $H_{mix}$ , and (F)  $N_a$ , and as a function of (G)  $L$  and (H)  $f_c$ . Points are hourly averages over the last hour of a 6-h simulation.  $A_c$  is calculated based on cloud optical depth  $\tau$  (32). Points are colored by  $L$ . In F, the slopes of the dashed lines indicate albedo susceptibility for given  $L$ . Slopes are steeper at small  $N_d$  and flatten with increasing  $N_d$ .

simple deterministic interactions between components of the system. Atmospheric Rayleigh–Bénard convection is one such example that links fundamental process to pattern. Emergence, or pattern formation, provides useful constraints on simulation of deterministic systems and opens rich opportunity for the pursuit of understanding pattern structure and its evolution.

This leads to yet another aspect of Newtonian/Darwinian merging, namely the development of simple, falsifiable models that can be tested in a range of conditions and locales. By illustrating the limits of physical determinism, the system of three coupled differential equations of ref. 23 has been particularly enlightening. This search for simplicity runs counter to the current trend toward ever-increasing model complexity—often to the point of attempting to represent complex interactions in models that do not adequately represent the individual components, let alone their interaction. Mixed layer models (24) and simple budget models (25) prove to be very useful, and are able, in some cases, to reproduce temporal (26) and spatial (27) emergence. By focusing on spatiotemporal patterns, the study of emergence naturally lends itself to simple models. Although this topic is of great interest, it will not be developed here.

Here we will attempt to balance Newtonian determinism and Darwinian (real-world system) complexity, particularly with an eye to scaling properties. The examples to be presented focus on albedo and radiative effect; precipitation is only discussed to the extent that it affects albedo. Simple models or computationally

efficient models will be alluded to, where appropriate. We start with a set of idealized numerical simulations using a cloud-resolving model (CRM) and a large eddy simulation (LES), and progress to discussion of a more ambitious project connected tightly to real-world simulation and observation.

## Results

**Simulations.** We use a numerical model, the System for Atmospheric Modeling (SAM) (28). To explore the robustness of the ( $A$ ,  $f_c$ ) relationship, we apply it to a variety of cases, including nocturnal marine stratocumulus (both closed and open cell), stratocumulus evolving with the diurnal cycle, and a stratocumulus to cumulus transition case. The simulations are separated into “nocturnal” and “diurnal” and described below.

**Marine stratocumulus: Nocturnal simulations.** These simulations focus on the sensitivity of cloud albedo  $A_c$ , cloud fraction  $f_c$ , and liquid water path  $L$  to the initial conditions; i.e., they directly address the question of CRE-controlling parameters without considering CRE itself. This is clearly unrealistic but will be used to make some salient points. The model output comprises 220 simulations of marine stratocumulus cloud systems. SAM is initiated with different initial conditions, described in terms of six key parameters: total mixing ratio  $q_t$ , liquid water potential temperature  $\theta_l$ , the depth of the mixed layer  $H_{mix}$  over which  $q_t$  and  $\theta_l$  are well mixed,  $q_t$  and  $\theta_l$  jumps at the inversion,  $\Delta q_t$  and  $\Delta\theta_l$ , and aerosol concentration  $N_a$ . The respective ranges of these

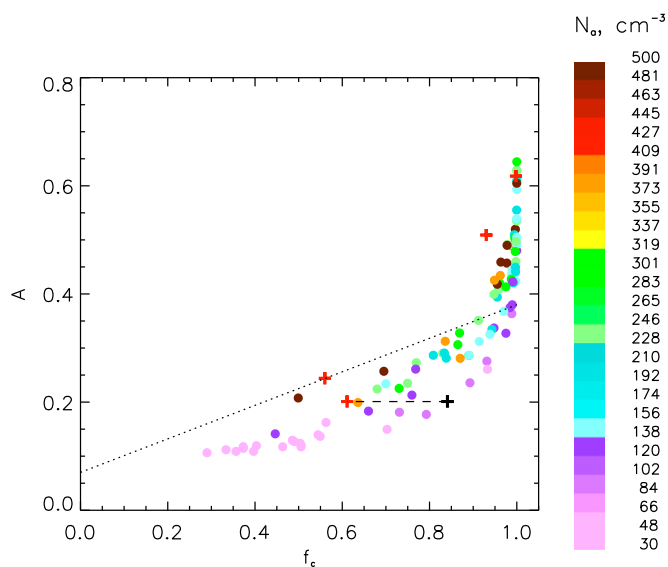


**Fig. 2.** Mean scene albedo  $A$  (cloudy plus clear sky) calculated based on Eq. 3 (with  $A_s = 0.08$ ) as a function of  $f_c$  (defined based on  $\tau > 0.2$ ). Points are colored by  $N_a$ . The aerosol influences both the cloud and surface albedo. A weak but distinct influence of  $N_a$  on  $A$  can be seen. Points associated with higher  $N_a$  tend to be at higher  $A$  and higher  $f_c$ . The dotted line is an approximation to the relationship in ref. 18 for  $2.5^\circ \times 2.5^\circ$  monthly average data from Californian stratocumulus (MODIS and CERES on Terra). The red “+” signs (not colored by  $N_a$ ) are from 3D radiative transfer calculations for four cloud fields associated with a closed-cell stratocumulus transitioning to the open-cell state (34), also with  $f_c$  defined based on  $\tau > 0.2$ . The black “+” sign is a recalculation of the red “+” to its left where a weaker condition ( $\tau > 0.1$ ) is applied to the calculation of  $f_c$ .

parameters are  $6.5 < q_t < 10.5 \text{ g}\cdot\text{kg}^{-1}$ ,  $284 < \theta_t < 294 \text{ K}$ ,  $-10 < \Delta q_t < -6 \text{ g}\cdot\text{kg}^{-1}$ ,  $6 < \Delta \theta_t < 10 \text{ K}$ ,  $500 < H_{mix} < 1,300 \text{ m}$ , and  $30 < N_a < 500 \text{ cm}^{-3}$ . Only those initial profiles sampled from the  $q_t$ ,  $\theta_t$ ,  $H_{mix}$  parameter space with  $L$  in the range 30–200  $\text{g}\cdot\text{m}^{-2}$  and cloud base in the range 250–1,100 m were selected for simulation. The parts of the parameter space excluded, which are dependent on a 3D combination of  $q_t$ ,  $\theta_t$ , and  $H_{mix}$ , are areas/combinations where the simulation would be very unlikely to produce the cloud type of interest. Hence, we do have some predetermined correlation between input parameters  $q_t$ ,  $\theta_t$ , and  $H_{mix}$ . The domain is  $40 \text{ km} \times 40 \text{ km} \times 1.6 \text{ km}$ , the grid volume is  $200 \text{ m} \times 200 \text{ m} \times 10 \text{ m}$ .

We perform two groups of simulations, each with a different method of sampling the initial conditions from the six-dimensional parameter uncertainty space that defines the parameter ranges and constraints. Each group of simulations is allowed to sample from the same ranges of the input parameters  $q_t$ ,  $\theta_t$ ,  $H_{mix}$ ,  $\Delta q_t$ ,  $\Delta \theta_t$ , and  $N_a$ . The first group of 100 simulations (set 1) was sampled randomly from a six-dimensional grid covering the meteorological and aerosol parameter space. About 40 of the 100 simulations apply the full range of  $N_a$  at fixed meteorology. The second group of 120 simulations (set 2) was sampled using the maximin Latin hypercube design algorithm (29). It maximizes the minimum distance between selected points to ensure optimal coverage of the multidimensional parameter space, which is difficult to obtain manually. Hence, a wider area of the multidimensional parameter space is covered in set 2 than in set 1. Unlike set 1, set 2 has no predetermined correlation between the meteorological drivers ( $q_t$ ,  $\theta_t$ ,  $H_{mix}$ ,  $\Delta q_t$ , and  $\Delta \theta_t$ ) and  $N_a$ .

Thus, the manner in which the six input parameters covary differs between the two sets. Because meteorology and aerosol typically covary in somewhat predictable ways, neither of the methods is a realistic sampling of what the atmosphere presents

(except for the realistic range over which the parameters are varied), but, as will be demonstrated below, they serve our purpose well.

**Marine stratocumulus and stratocumulus-to-trade cumulus transition: Diurnal simulations.** Here the focus is on CRE,  $A$ , and  $f_c$ . A random sample of 15 of the 220 nocturnal simulations are repeated for a period of 10 h with a 04:00 local time start time and a diurnal cycle of radiation. Radiative calculations are applied in each model column. In addition, a composite sounding based on NE Pacific Lagrangian trajectories (30) is used to simulate a transition case in the presence of (absorbing) smoke aerosol residing some distance above, and later entrained into cloud. Forcings, including a gradual increase in sea surface temperature, are applied (30). For this transition case, the SW heating associated with the aerosol is also coupled to dynamics (31). A solid stratocumulus to broken cumulus transition is simulated over the course of 3 d; initial smoke conditions are either low  $N_a$  (aerosol optical depth  $\tau_a = 0.06$ ) or high  $N_a$  ( $\tau_a = 0.50$ ). The asymmetry parameter is 0.67, and the single scattering albedo  $\omega_o$  is 0.80 (at 0.5  $\mu\text{m}$ ), representing smoke mixed with hygroscopic material (31). Such a low value of  $\omega_o$  is associated with fresh smoke and is perhaps unrealistic. It does, however, serve to test the sensitivity of the ( $A$ ,  $f_c$ , CRE) phase space to aerosol absorption. The model is run on a  $12 \text{ km} \times 12 \text{ km} \times 4 \text{ km}$  domain with a grid volume of  $50 \text{ m} \times 50 \text{ m} \times 10 \text{ m}$ .

### Simulation Results.

**Marine stratocumulus: Nocturnal simulations.** A scatterplot of the domain mean cloud albedo  $\bar{A}_c$  as a function of the six input parameters is shown in Fig. 1 for set 1. Each point represents an hourly average over hour 6 of the simulation, and is colored by  $L$ .  $\bar{A}_c$  is calculated from  $\tau$  using a two-stream approximation (32). Ignoring the coloring by  $L$ , one immediately sees that there is no simple dependence of  $\bar{A}_c$  on individual parameters. Sorting by  $L$  does bring out some distinct patterns, which is particularly clear for  $\bar{A}_c$  vs.  $N_a$ . This is an expression of the albedo susceptibility relationship, calculated at constant  $L$ :  $S_a = \partial \bar{A}_c / \partial N_a = A_c(1 - A_c) / 3N_a$  (33); slopes for given  $L$  in Fig. 1F are maximum at small  $N_a$  and  $\bar{A}_c \approx 0.5$ .  $\bar{A}_c$  is also shown to depend strongly on  $L$  and  $f_c$  (Fig. 1G and H). A partial multivariate linear correlation of  $\bar{A}_c$  vs. the six input parameters (i.e., a correlation between  $\bar{A}_c$  and any one of the six parameters with the effects of the others removed) produces correlation coefficients of 0.44 ( $q_t$ ),  $-0.56$  ( $\theta_t$ ), 0.58 ( $H_{mix}$ ),  $-0.32$  ( $\Delta q_t$ ), 0.35 ( $\Delta \theta_t$ ), and 0.67 ( $\ln N_a$ ). Thus, all input parameters contribute significantly to  $\bar{A}_c$ .

We now calculate  $A$  as in Eq. 3 with  $A_s = 0.08$  (for ocean), and  $A_c$  and  $f_c$  based on  $\tau > 0.2$  (chosen for consistency with 3D calculations in Fig. 2). Points are domain average values, colored by input  $N_a$ . One sees (Fig. 2) a weak but distinct separation of colors, indicating that, for given  $f_c$ , higher  $N_a$  tends to result in higher  $A$ . Fig. 2 also includes calculations based on 3D radiative transfer modeling of four individual snapshots of cloud fields from an independent simulation (four red “+” signs) (34). The location of these points is close to those from the two-stream approximation, suggesting that details of the  $A$  calculation appear to have a small influence. There is, however, a distinct sensitivity to the definition of  $f_c$ : the red “+” signs calculate  $f_c$  based on  $\tau > 0.2$ , whereas the black “+” sign calculates  $f_c$  for  $\tau > 0.1$ .

A line approximating monthly mean  $2.5^\circ \times 2.5^\circ$  results for a MODIS Terra measurement from Californian stratocumulus (18) is superimposed on Fig. 2 for reference. Except for the bounding by  $A_s$  at  $f_c = 0$  and by  $A_c$  at  $f_c = 1$ , there is no a priori reason why the relationship based on the small spatiotemporal averaging in this work should behave similarly to that from the large spatiotemporal averaging as in ref. 18; differences between the CRM output and the remote sensing data are likely related, among others, to the averaging scale, covariability in meteorology and aerosol, and definition of  $f_c$  (Fig. S1). The relative

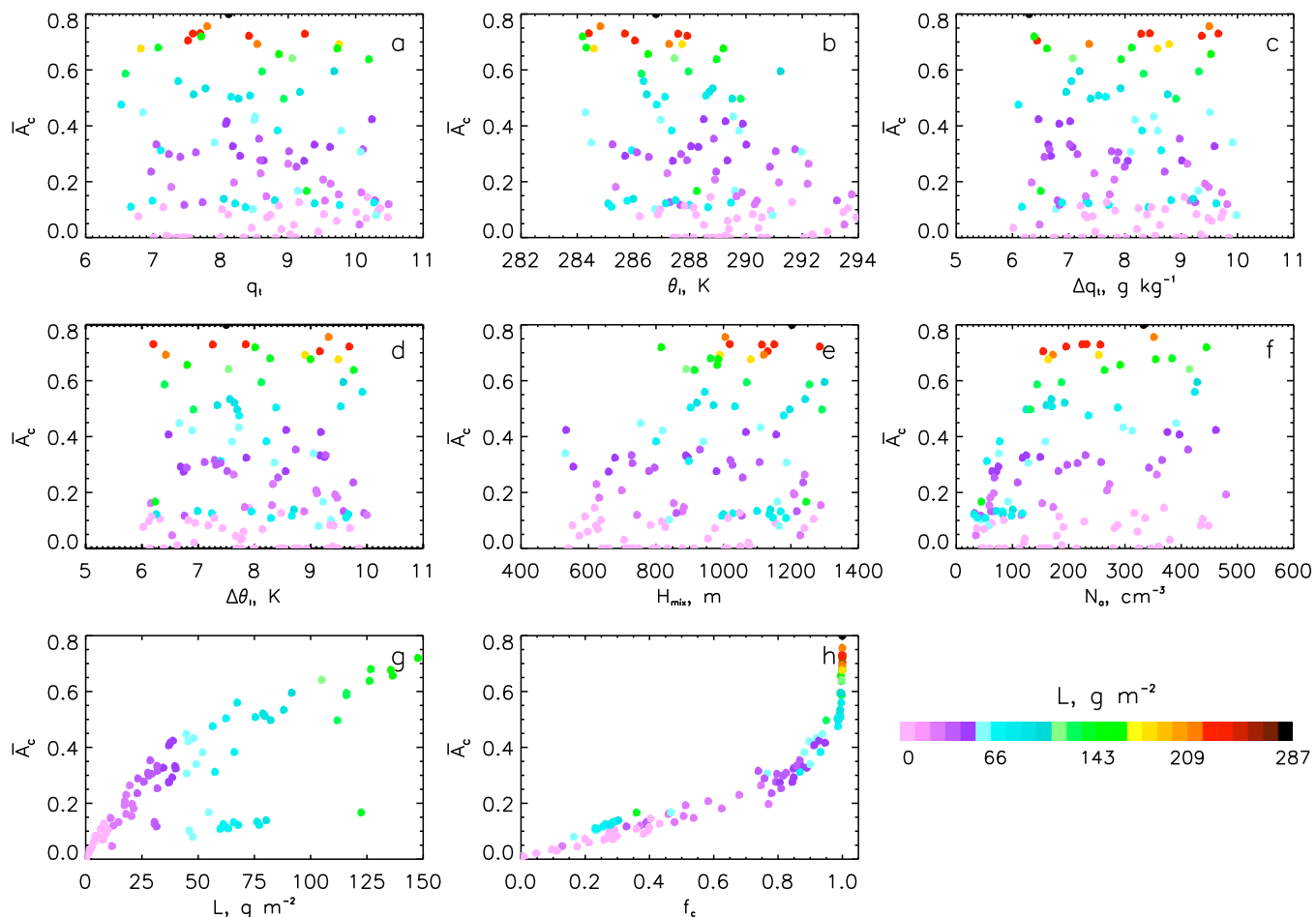


Fig. 3. As in Fig. 1 but for set 2.

robustness of the  $(A, f_c)$  relationship reinforces our point that well-defined higher-level relationships are preferred over uncertain, poorly constrained lower-level ones. Efforts to understand the connection between the form of the  $(A, f_c)$  relationship and its controlling factors would therefore seem profitable.

Figures for set 2 show similar behavior for the scatter plots in terms of the individual inputs (Fig. 3). The robust relationships are again reflected in  $\bar{A}_c$  vs.  $L$  and  $f_c$ . Applying Eq. 3, the  $A$  vs.  $f_c$  relationship is highlighted again (Fig. 4), this time with  $f_c$  and  $A_c$  based on  $\tau > 1$ . Here, there is almost no discernible influence of  $N_a$  on  $A$  at constant  $f_c$ , regardless of how  $f_c$  and  $A_c$  are defined (see *SI Text* and Fig. S2). Moreover, both high and low  $N_a$  are intermingled over a range of  $A$  and  $f_c$ . Although these two sets of simulations sample from the same range of initial conditions, they differ (i) in the manner in which the six input parameters are sampled and (ii) in the parameter space covered by the sampling. Unlike set 1, there is almost no repetition of meteorological conditions defined by the input combinations in the set 2 simulations. This brings out an important point: The influence of the aerosol on albedo at constant  $f_c$  depends on the covariability of meteorology and aerosol. This is a result supported by observational studies that have underscored the difficulty in separating meteorological and aerosol influences on  $A$  because variability in  $A$  is overwhelmed by variability in  $f_c$  and  $L$  (21). The  $(A, f_c)$  phase space is a useful way of demonstrating this, and there is a clear need for realism in the sampling of the covarying initial conditions if we are to discern aerosol influences. The frequently used modeling strategy where  $N_a$  is varied for given

meteorology should not be applied, and demonstration of an aerosol response in this framework is not an indication of realistic response, unless, of course, nature presents such conditions.

It is worth noting that low  $N_a$  is often associated with precipitation-induced cloud breakup. Thus, to the extent that  $N_a$  controls precipitation in these systems, it has the potential to strongly affect  $A$  and  $f_c$  by moving points toward the lower left of the  $(A, f_c)$  trace. Here too, differences between set 1 and set 2 are distinct; in Fig. 2, points with low  $N_a$  and low  $f_c$  are more common than in Fig. 4.

**Marine stratocumulus and stratocumulus-to-trade cumulus transition: Diurnal simulations.** These simulations include part of the diurnal cycle so that the broadband SW CRE can be calculated over the course of 10 h for the stratocumulus simulations and 3 d for the transition cases. To simplify analysis, we calculate relative CRE (rCRE),

$$\text{rCRE} = 1 - \frac{F_{sw,all}}{F_{sw,clr}} \quad [4]$$

where  $F_{sw}$  denotes net SW surface fluxes, *all* denotes all sky, and *clr* denotes clear sky. Measurement of rCRE was developed for surface-based measurements (19) and, by normalizing, focuses on clouds, without the confounding effects of solar angle or surface albedo.

Here rCRE calculations are performed based on Eq. 4 during daylight hours when SW fluxes are calculated. The rCRE is shown as a function of  $f_c$  (based on  $\tau > 1$ ; Fig. 5A) and scene albedo  $A$  (Fig. 5B) for the composite of 15 stratocumulus (1-h

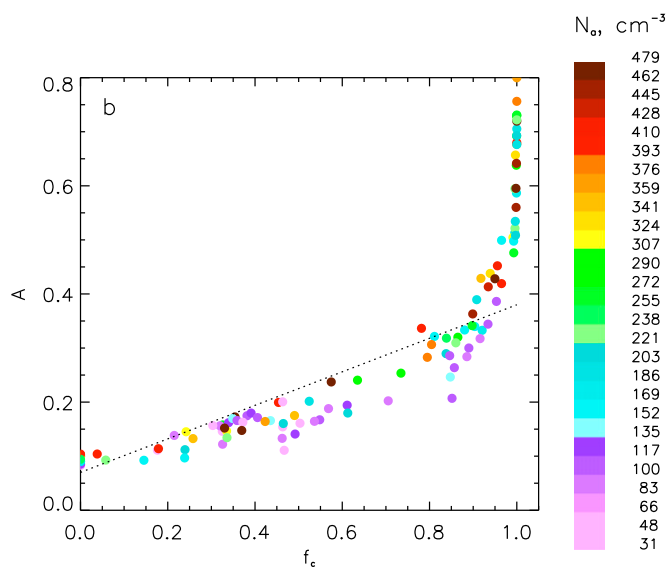


Fig. 4. As in Fig. 2 but for set 2. Here  $f_c$  and  $A_c$  are calculated based on  $\tau > 1$ . Note the absence of a clear aerosol influence on  $A$  and  $f_c$ .

snapshots) and 2 transition simulations (low  $\tau_a$  and high  $\tau_a$ ), also at hourly intervals. Such analyses show the relative importance of intrinsic factors ( $A$ ) or extrinsic factors ( $f_c$ ) in controlling rCRE (20, 22). It is immediately clear that the simulations tend to follow a fairly robust relationship, with rCRE, as expected, increasing progressively with increasing  $f_c$  and  $A$ . The low  $\tau_a$  transition case output (filled circles) follows the stratocumulus (filled squares) cases quite well despite the large differences in initial soundings and system evolution. The points from the high  $\tau_a$  smoky transition case tend to lie below the main branch of stratocumulus points (Fig. 5B, diamonds); at low  $f_c$ , they illustrate the brightening of the dark ocean surface by the aerosol. The few scattered (diamond) points at the very highest rCRE and  $A$  are associated with smoke-influenced clouds with very high  $N_a$  and  $N_d$ .

Model output from Fig. 5A and B, this time in ( $A$ ,  $f_c$ ) phase space with points colored by rCRE (Fig. 5C), again shows the characteristic path in ( $A$ ,  $f_c$ ) space. Note that points with similar  $A$  and  $f_c$  may have significantly different rCRE because they are associated with different cloud and aerosol conditions. Although we make no claims on the universality of relationships such as those in Fig. 5, the robustness suggests that the ( $A$ ,  $f_c$ ) phase space is a useful one for exploring controls on rCRE (or CRE) and linking physical processes and assumptions made in the analysis to rCRE patterns.

### A Path Forward

**The Primacy of Initial Conditions.** Results emphasize the influence of the covariability (in six-dimensional space) of initial conditions/cloud-controlling parameters on key cloud field attributes. Two sampling strategies from the same range of initial conditions produce different indications of the role of the aerosol. This leads to the question of how the system might respond to a naturally occurring covariability of the inputs. We propose to address this question by repeating large numbers of LES, CRM, and coarser mesh model simulations in specified cloud regimes using initial conditions from routine observations (or observationally constrained model output), as in ref. 35, but also including aerosol information. Initial conditions could be based on radiosondes or from reanalysis, daily Numerical Weather Prediction (NWP) derived soundings, or variational analysis (36). Model output that successfully reproduces a desired set of observed quantities, which should include surface SW radiation,  $L$ ,  $f_c$ , and

$A_c$ , can then be tied to the observed initial meteorological conditions,  $N_a$ , and surface latent and sensible heat fluxes. [“Successful” is defined ad hoc. For a radiation-centric study, a successful simulation would need to compare sufficiently well to

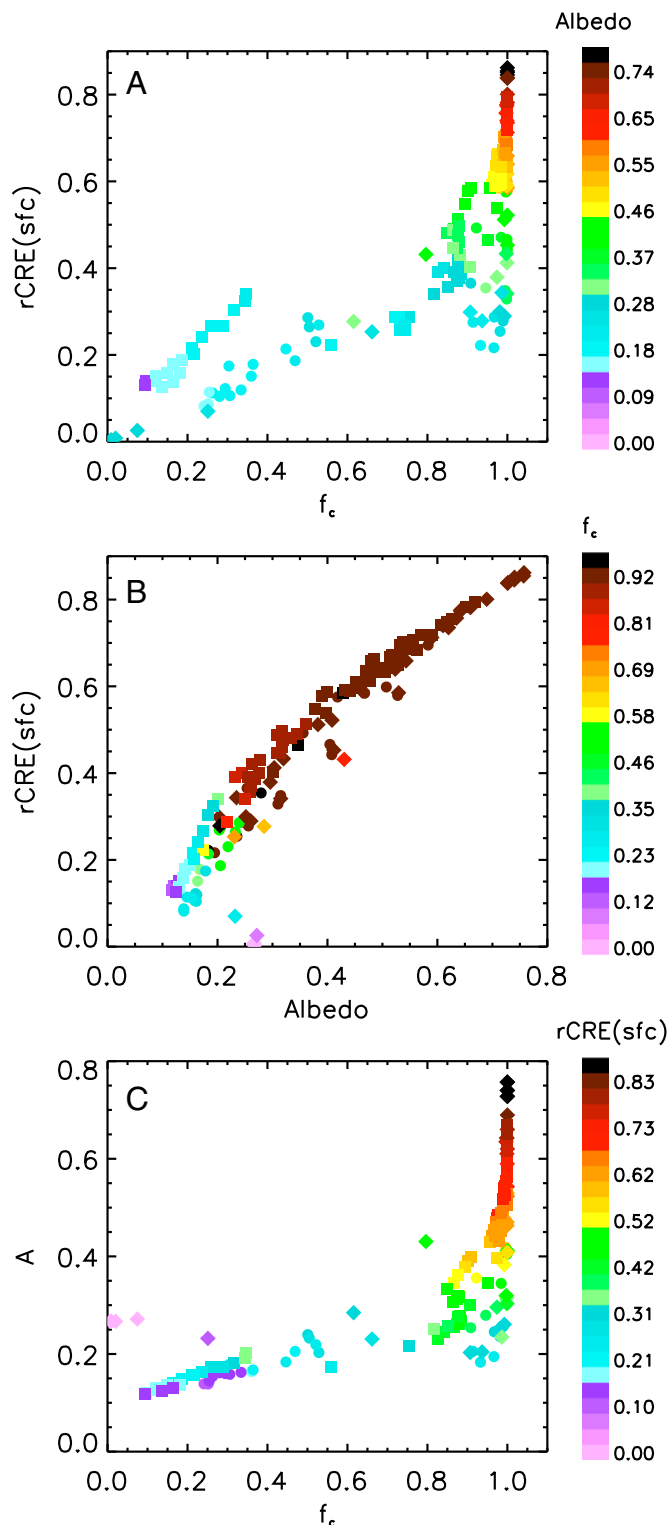
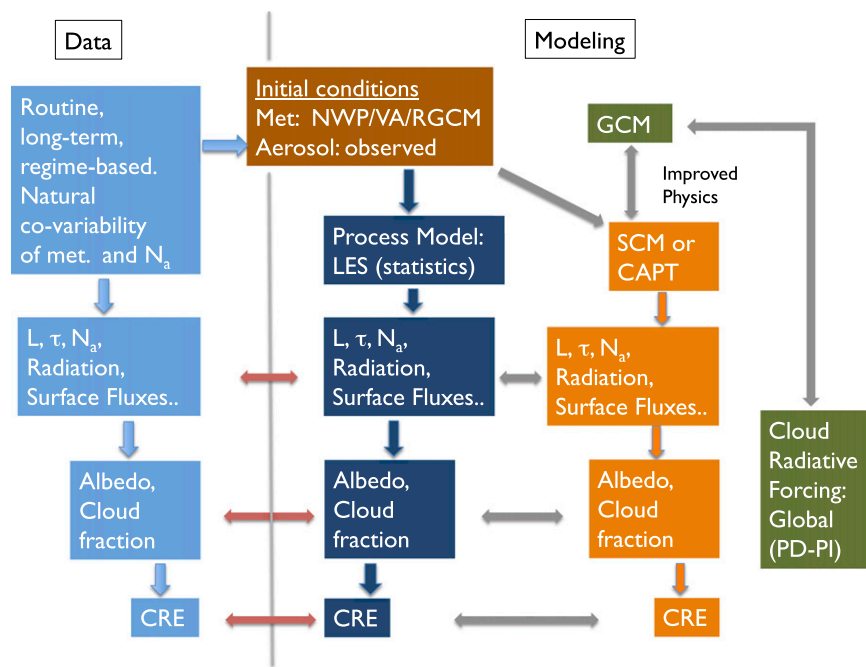


Fig. 5. The rCRE calculations in (albedo  $A$ ,  $f_c$ ) space for 15 stratocumulus and 2 stratocumulus-to-trade-cumulus transition simulations: (A) rCRE vs.  $f_c$ ; (B) rCRE vs. albedo  $A$ , and (C) albedo  $A$  vs.  $f_c$ . Squares, stratocumulus; circles, low smoke  $\tau_a$  transition case; diamonds, high smoke  $\tau_a$  transition case. Points represent 1-h snapshots. Here  $f_c$  and  $A_c$  are calculated based on  $\tau > 1$ .



**Fig. 6.** Schematic showing systematic comparison between surface and/or satellite remote sensing of key measurements with those produced by high-resolution LES and/or SCM output. Here the focus is on high-level parameters such as  $A$ ,  $f_c$ , and CRE, but more detailed comparisons at the level of  $L$ ,  $\tau$ ,  $r_e$ ,  $N_a$ , and surface fluxes provide further physical consistency checks. The LES and SCM are driven, on a routine basis, by realistic initial conditions that capture the natural covariability of aerosol and meteorology. Systematic improvements in SCMs provide a pathway to improved AGCM physics so that climate-relevant present-day (PD) minus preindustrial (PI) calculations can be performed. AGCMs run in hindcast mode with the same input conditions can also be used. CAPT, Cloud-Associated Parameterizations Testbed (39); VA, Variational Analysis; RGCM, Regional General Circulation Model.

measurements of, *inter alia*, surface SW radiation,  $\tau$ ,  $f_c$ , and  $L$ . As in ref. 37, the unsuccessful simulations provide opportunity for model improvement (both LES and SCM.) Given that observed profiles will differ from the idealized mixed layer profiles used here, classification of observed profiles in terms of key characteristics will likely be necessary. A large number of simulations will then allow one to explore the relationship between input profiles and CRE,  $A_c$ ,  $f_c$ ,  $L$ , and  $N_a$ .

Analyses of successful model output in (CRE,  $A$ ,  $f_c$ ) space will allow a methodical, process-based link to observed environmental and aerosol conditions with a hierarchy of models but, importantly, will include small-scale process models. Because individual microphysical and macrophysical responses to the aerosol can also be measured from the surface and from satellites, there is benefit in examining, in parallel, individual response terms  $d \ln X / d \ln N_a$  (e.g., Eq. 2) and comparing model output and observations at multiple levels. Agreement at multiple levels will provide further confidence in the fidelity of simulations. Nevertheless, we urge appropriate balance in these higher- and lower-order efforts, given the measurement uncertainties and imperfect model physics.

Routine LES has been demonstrated for improving single-column model (SCM) physics, thus providing a direct path to improving AGCM physics (37). The US Department of Energy's Atmospheric Radiation Measurement Program will soon embark on a pilot study to perform routine LES at the Southern Great Plains site in Oklahoma (38), and a European project (High Definition Clouds and Precipitation for Climate Prediction; [www.hdcp2.eu/](http://www.hdcp2.eu/)) has similar goals of routine, integrated modeling and observation. In addition to SCM simulations, AGCMs could directly benefit if they are initialized with the same inputs and run in hindcast mode over short periods of time (39). A schematic of the approach is shown in Fig. 6. This effort should be performed in key cloud regimes such as stratocumulus, cumulus, and the stratocumulus-to-cumulus transition. For deep convective clouds, CRE calculations require other considerations.

**Emulators.** LES, and even CRM, is computationally expensive, so pursuit of a physically or perhaps statistically based simpler model with a limited number of free parameters is of great interest. These simpler representations would be designed to emulate LES or CRM results and explain the sensitivities of key outputs such as  $A_c$ ,

$f_c$ , CRE, and  $L$  to the initial conditions. Simplified budget models and statistically based emulators (40, 41) have been proposed. The two aforementioned studies assessed the uncertainty of key model outputs with respect to uncertainty in model parameters representing physical processes. Rather than assess sensitivity to model parameters, here the emulator will be used to relate variations in  $A$ ,  $f_c$ , and CRE to meteorological and aerosol drivers. The construction of an emulator requires optimal coverage of the parameter space in the sample of model runs using, e.g., the maximin Latin hypercube approach (hence the use of this sampling method for set 2; Figs. 3 and 4). These 120 simulations are currently being used to construct emulators, and are showing promise. The greatest challenge is the sometimes steep local slope in six-dimensional input parameter space, meaning that small changes in input parameters have a large influence on the outcome. A successful emulator would ultimately use as input the observed covarying initial conditions and would, at minimal computational expense, allow a much denser sampling of parameter space than the LES or CRM. Emulators would have to be reconstructed for different cloud regimes. To the extent that this experiment is successful, emulation could serve as a very useful method for relating initial conditions to CRE,  $A$ , and  $f_c$  outcomes in different cloud regimes. Moreover, the output parameters are all measurable, which means that the emulator could be tested against observations in parts of the input space not used to train the emulators.

### Summary

The proposed analysis framework combines our penchant for Newtonian determinism in the form of cloud system modeling, that resolves key physics, addresses scale dependence, seeks emergent phenomena, and pursues simple models, with the Darwinian recognition that our system is fundamentally unpredictable and cannot be addressed purely deterministically. The approach shifts the balance of effort from low-order observational constraints, that are highly scale-dependent and suffer from instrumental or retrieval error, toward constraints on higher-order parameters that are fundamental to the CRE. The latter, expressed here as an ( $A$ ,  $f_c$ ) relationship and  $CRE = f(A, f_c)$ , are not without uncertainty, but, by addressing them at this higher level, we avoid excessive compounding or unwanted offsetting of errors.

Numerical simulation of warm cloud systems has been used to demonstrate that the manifestation of aerosol effects on  $A$  and  $f_c$  depends on the covariability of meteorology and aerosol. We note, however, that, even when aerosol effects on albedo at constant  $f_c$  are overwhelmed by other factors (e.g., Fig. 4), aerosol effects on precipitation may still provide a strong control on  $A$  and  $f_c$  (34), and this avenue for the radiative effect of the aerosol still appears to be pivotal. The  $(A, f_c)$  trajectories have been shown to be relatively robust, but they show some sensitivity to covariability of initial conditions, meteorological regime, and averaging scale. Their scaling properties therefore deserve attention. They are also sensitive to the definition of  $f_c$  (Fig. 2 and *Supporting Information*), an issue raised in various other works (42). Analyses should therefore always be associated with clear criteria for definition of  $f_c$ .

We amplify the call for routine LES driven by observed simultaneously varying meteorological and aerosol conditions to clarify the relationship between covariability in aerosol and meteorology and the  $(A, f_c)$  CRE phase space in a process model framework. Current efforts at elucidating this relationship rely on reanalysis (21, 22), and although the latter approach is valuable at the regional circulation scale, reanalysis is not reliable enough at the cloud scale. Model–observation comparison at the level of individual microphysical and macrophysical responses to the aerosol (Eq. 2) will provide further confidence in the fidelity of simulations.

As noted elsewhere (37), routine LES provides a mechanism to rigorously evaluate models against a desired set of output

parameters. Successful simulations (based on prescribed tolerances) form an observationally constrained model output, which could be used for multiple other analyses similar to the various Model Intercomparison projects.

One of the tenets of the merging of Newtonian and Darwinian worldviews somewhat neglected here is the development of simple models. This merging is itself recognition of the imperfection of Popper's "clocks." Lorenz's model (23) epitomizes the merged approach because it not only captures the spirit of the merging but also highlights the imperfection of the clock through its identification of sensitivity to initial conditions. Statistical emulator models are far from simple, and do not provide process level understanding like a simple model does. However, when designed with, and driven by, the appropriate regime-based conditions, they may be an expedient and pragmatic tool for filling in gaps and extending our ability to represent the aerosol–cloud system in different regimes. Simple, transparent models (8, 43) should be considered in parallel.

**ACKNOWLEDGMENTS.** The authors thank the Sackler Colloquium for the opportunity to present these ideas. Funding was provided by NOAA's Climate Goal and the US Department of Energy, Office of Science, Biological and Environmental Research under the Atmospheric System Research Program (Grants DE-SC0006972 and DE-SC0008112). We acknowledge funding from the UK Natural Environment Research Council ACID-PRUF (Aerosol-Cloud Interactions - A Directed Programme to Reduce Uncertainty in Forcing) Grant NE/I020059/1.

- Stevens B, Feingold G (2009) Untangling aerosol effects on clouds and precipitation in a buffered system. *Nature* 461(7264):607–613.
- Twomey S (1977) The influence of pollution on the shortwave albedo of clouds. *J Atmos Sci* 34(7):1149–1152.
- Albrecht BA (1989) Aerosols, cloud microphysics, and fractional cloudiness. *Science* 245(4923):1227–1230.
- Lee S-S, Feingold G, Chuang PY (2012) Effect of aerosol on cloud–environment interactions in trade cumulus. *J Atmos Sci* 69(12):3607–3632.
- Parodi A, Fofoula-Georgiou E, Emanuel K (2011) Signature of microphysics on spatial rainfall statistics. *J Geophys Res* 116(D14):D14119.
- Bollasina MA, Ming Y, Ramaswamy V (2011) Anthropogenic aerosols and the weakening of the South Asian summer monsoon. *Science* 334(6055):502–505.
- Lau K-M, Kim M-K, Kim K-M (2006) Asian summer monsoon anomalies induced by aerosol direct forcing: The role of the Tibetan Plateau. *Clim Dyn* 26(7):855–864.
- Harte J (2002) Towards a synthesis of the Newtonian and Darwinian worldviews. *Phys Today* 55:29–34.
- Popper KR (1966) *Of Clocks and Clouds: An Approach to the Problem of Rationality and the Freedom of Man. The Arthur Holly Compton Memorial Lecture* (Washington Univ, St. Louis).
- Wood R (2007) Cancellation of aerosol indirect effects in marine stratocumulus through cloud thinning. *J Atmos Sci* 64(7):2657–2669.
- Ghan S, et al. (2016) Challenges in constraining anthropogenic aerosol effects on cloud radiative forcing using present-day spatiotemporal variability. *Proc Natl Acad Sci USA* 113:5804–5811.
- Taylor KE, et al. (2007) Estimating shortwave radiative forcing and response in climate models. *J Clim* 20(11):2530–2543.
- Penner JE, Xu L, Wang M (2011) Satellite methods underestimate indirect climate forcing by aerosols. *Proc Natl Acad Sci USA* 108(33):13404–13408.
- Ackerman AS, et al. (2000) Effects of aerosols on cloud albedo: Evaluation of Twomey's parameterization of cloud susceptibility using measurements of ship tracks. *J Atmos Sci* 57(16):2684–2695.
- McComiskey A, Feingold G (2012) The scale problem in quantifying aerosol indirect effects. *Atmos Chem Phys* 12(2):1031–1049.
- Charlock TP, Ramanathan V (1985) The albedo field and cloud radiative forcing produced by a general-circulation model with internally generated cloud optics. *J Atmos Sci* 42(13):1408–1429.
- Webb M, Senior C, Bony S, Morcrette JJ (2001) Combining ERBE and ISCCP data to assess clouds in the Hadley Centre, ECMWF and LMD atmospheric climate models. *Clim Dyn* 17(12):905–922.
- Bender FA-M, Charlson RJ, Ekman AML, Leahy V (2011) Quantification of monthly mean regional-scale albedo of marine stratiform clouds in satellite observations and GCMs. *J Appl Meteorol Climatol* 50(10):2139–2148.
- Betts AK (2007) Coupling of water vapor convergence, clouds, precipitation, and land-surface processes. *J Geophys Res* 112(D10):D10108.
- Xie Y, Liu Y (2013) A new approach for simultaneously retrieving cloud albedo and cloud fraction from surface-based shortwave radiation measurements. *Environ Res Lett* 8:044023.
- George RC, Wood R (2010) Subseasonal variability of low cloud radiative properties over the southeast Pacific Ocean. *Atmos Chem Phys* 10(8):4047–4063.
- Chen Y-C, Christensen MW, Stephens GL, Seinfeld JH (2014) Satellite-based estimate of global aerosol-cloud radiative forcing by marine warm clouds. *Nat Geosci* 7:643–646.
- Lorenz EN (1963) Deterministic nonperiodic flow. *J Atmos Sci* 20(2):130–141.
- Lilly DK (1968) Models of cloud-topped mixed layers under a strong inversion. *Q J R Meteorol Soc* 94(401):292–309.
- Wood R, Leon D, Lebock M, Snider J, Clarke AD (2012) Precipitation driving of droplet concentration variability in marine low clouds. *J Geophys Res* 117(D19):D19210.
- Koren I, Feingold G (2011) Aerosol–cloud–precipitation system as a predator-prey problem. *Proc Natl Acad Sci USA* 108(30):12227–12232.
- Feingold G, Koren I (2013) A model of coupled oscillators applied to the aerosol–cloud–precipitation system. *Nonlinear Process Geophys* 20(6):1011–1021.
- Khairoutdinov MF, Randall DA (2003) Cloud resolving modeling of the ARM summer 1997 IOP: Model formulation, results, uncertainties, and sensitivities. *J Atmos Sci* 60(4):607–625.
- Morris MD, Mitchell TJ (1995) Exploratory designs for computer experiments. *J Stat Plan Inference* 43:381–402.
- Sandu I, Stevens B (2011) On the factors modulating the stratocumulus to cumulus transitions. *J Atmos Sci* 68(9):1865–1881.
- Feingold G, Jiang H, Harrington JY (2005) On smoke suppression of clouds in Amazonia. *Geophys Res Lett* 32(2):L02804.
- Bohren CF (1987) Multiple scattering of light and some of its observable consequences. *Am J Phys* 55(6):524–533.
- Platnick S, Twomey S (1994) Determining the susceptibility of cloud albedo to changes in droplet concentration with the Advanced Very High Resolution Radiometer. *J Appl Meteorol* 33(3):334–347.
- Feingold G, Koren I, Yamaguchi T, Kazil J (2015) On the reversibility of transitions between closed and open cellular convection. *Atmos Chem Phys* 15(13):7351–7367.
- Seifert A, Köhler C, Beheng KD (2012) Aerosol-cloud-precipitation effects over Germany as simulated by a convective-scale numerical weather prediction model. *Atmos Chem Phys* 12(2):709–725.
- Zhang MH, Lin JL, Cederwall RT, Yio JJ, Xie SC (2001) Objective analysis of the ARM IOP data: Method and sensitivity. *Mon Weather Rev* 129(2):295–311.
- Neggers RAJ, Siebesma AP, Heus T (2012) Continuous single-column model evaluation at a permanent meteorological supersite. *Bull Am Meteorol Soc* 93(9):1389–1400.
- U.S. Department of Energy (2014) *Atmospheric Radiation Measurement Climate Research Facility – Atmospheric System Research High-Resolution Modeling Workshop* (US Dep Energy, Washington, DC), DOE/SC-0169.
- Phillips TJ, et al. (2004) Evaluating parameterizations in General Circulation Models: Climate simulation meets weather prediction. *Bull Am Meteorol Soc* 85(12):1903–1915.
- Carslaw KS, et al. (2013) Large contribution of natural aerosols to uncertainty in indirect forcing. *Nature* 503(7474):67–71.
- Johnson JS, et al. (2015) Evaluating uncertainty in convective cloud microphysics using statistical emulation. *J Adv Model Earth Syst* 7(1):162–187.
- Charlson RJ, Ackerman AS, Bender FA-M, Anderson TL, Liu Z (2007) On the climate forcing consequences of the albedo continuum between cloudy and clear air. *Tellus B Chem Phys Meteorol* 59(4):715–727.
- Stevens B (2015) Rethinking the lower bound on aerosol radiative forcing. *J Clim* 28(12):4794–4819.